AJNR Am J Neuroradiology 21:1785–1792, November/December 2000

CSF Flow Measurement in Syringomyelia

Pierre Brugières, Ilana Idy-Peretti, Clément Iffenecker, Fabrice Parker, Odile Jolivet, Michel Hurth, André Gaston, and Jacques Bittoun

BACKGROUND AND PURPOSE: **CSF circulation has been reported to represent a major factor in the pathophysiology of syringomyelia. Our purpose was to determine the CSF flow patterns in spinal cord cysts and in the subararachnoid space in patients with syringomyelia associated with Chiari I malformation and to evaluate the modifications of the flow resulting from surgery.**

METHODS: **Eighteen patients with syringomyelia were examined with a 3D Fourier encoding velocity imaging technique. A prospectively gated 2D axial sequence with velocity encoding in the craniocaudal direction in the cervical region was set at a velocity of ± 10 cm/s. Velocity measurements were performed in the larger portion of the cysts and, at the same cervical level, in the pericystic subarachnoid spaces. All patients underwent a surgical procedure involving dural opening followed by duroplasty. Pre- and postoperative velocity measurements of all patients were taken, with a mean follow-up of 10.2 months. We compared the velocity measurements with the morphology of the cysts and with the clinical data. Spinal subarachnoid spaces of 19 healthy subjects were also studied using the same technique.**

RESULTS: **A pulsatile flow was observed in syrinx cavities and in the pericystic subarachnoid spaces (PCSS). Preoperative maximum systolic cyst velocities were higher than were diastolic velocities. A systolic velocity peak was well defined in all cases, first in the cyst and then in the PCSS. Higher systolic and diastolic cyst velocities are observed in large cysts and in patients with a poor clinical status. After surgery, a decrease in cyst volume (evaluated on the basis of the extension of the cyst and the compression of the PCSS) was observed in 13 patients. In the postoperative course, we noticed a decrease of systolic and diastolic cyst velocities and a parallel increase of systolic PCSS velocities. Diastolic cyst velocities correlated with the preoperative clinical status of the patients and, after surgery, in patients with a satisfactory foraminal enlargement evaluated on the basis of the visibility of the cisterna magna.**

CONCLUSION: **CSF flow measurement constitutes a direct evaluation for the follow-up of patients with syringomyelic cysts. Diastolic and systolic cyst velocities can assist in the evaluation of the efficacy of surgery.**

Syringomyelia is associated with a number of abnormalities including Chiari I malformation, spinal trauma, spinal cord tumors, and arachnoiditis. Numerous theories of the pathophysiology of syringomyelia have been proposed (1–4), the most popular one being an obstruction of the spinal CSF pathways with resultant formation and extension of syringomyelic cysts (1, 5). CSF normally flows within the spinal cord along perivascular spaces to the central canal (6, 7), and it has been recently postulated that variation of patency of the central canal may play an important role in the development of syringomyelia (8).

Quantification of flow by MR imaging has already been used for in vivo flow measurements in vascular structures (9–13). MR imaging has also been used to investigate CSF circulation in the aqueduct and the normal flow pattern of CSF in the subarachnoid spaces (14–25). More recently, a semiquantitative approach of CSF flow with phase-contrast imaging has been proposed in patients with Chiari I malformations (26, 27).

The goal of our study was to determine quantitatively the flow pattern in syringomyelia and in the pericystic subarachnoid spaces (PCSS) and to evaluate changes in flow induced by surgery.

Methods

We examined 18 patients (seven men, 11 women; mean age = 41.8 years, SD = 16.2 years) with syringomyelia associated

Received July 14 1999; accepted after revision May 25, 2000.

From the Centre Inter-Etablissements de Recherche en Résonance Magnétique C.I.E.R.M. (P.B., J.B., O.J., I.I-P.), the Department of Neurosurgery (F.P., M.H.) of Bicêtre Hospital, Paris Sud University, and the Department of Neuroradiology (P.B., A.G.) of Henri Mondor Hospital, Université Paris Val de Marne.

Address reprint requests to Pierre Brugières, Department of Neuroradiology, Henri Mondor Hospital, 51 ave du Mal de Lattre de Tassigny 94000 Créteil, France.

with a Chiari I malformation and 19 healthy volunteers (10 men, nine women, mean age = 24.5 ± 3.5 years). In the volunteer group, we measured CSF velocities in the subarachnoid spaces at C3 and C5 levels, respectively. All the patients included in the study underwent an MR velocity study and a clinical grading and a morphologic evaluation of the cyst extension in the pre- and postoperative periods. All the patients underwent a surgical decompression at the foramen magnum performed in the same institution by two neurosurgeons (MH, FP). The surgical procedure entailed dural opening followed by duroplasty. Permeability of the foramen of Magendie was systematically controlled. When encountered, adhesions from the tonsils to the dura were lysed.

MR measurements were performed on a 1.5-T system using a cervical neck coil. A T1-weighted sequence (600/20 [TR/TE]; slice thickness, 4 mm; matrix, 256 × 128) was performed in the sagittal plane. Axial slices perpendicular to the posterior wall of each cervical spinal segment were secondarily obtained with the same parameters. Three to four axial planes focused on the largest part of the cyst were selected for the study of the CSF flow. A prospectively gated 2D axial gradient-recalled acquisition into steady state sequence with velocity encoding in the craniocaudal direction and flow sensitivity set to ± 10 cm/s was acquired at the levels of interest. Section thickness was 5 mm and the field of view was 160 × 160 mm with a 128 × 256 matrix. TE was set to 21 ms and a 40° flip angle was chosen because it represents a good compromise between a satisfactory flow-related enhancement and a sufficient stationary proton versus moving proton contrast. Pulse sequence was triggered with the R-wave of the ECG and 9 to 12 frames were obtained during every heart cycle. The minimum data acquisition delay after the R-wave was 13 ms, and the acquisitions were equally spaced through the first 80% of the RR interval. TR was dependent on patient heart rate, and varied from 60 to 80 ms. Both magnitude and phase images were obtained. Measurements were achieved by means of a 3D Fourier encoding velocity imaging (FEVI) technique with four encoding steps of a bipolar gradient and a zero-filling interpolation previously described (28). The resulting velocity maps were represented by use of a colored scale superimposed on the magnitude images, making a composite image. Caudocranial velocities were represented in blue (dark blue for slow velocities and light blue for higher velocities) and the representation of craniocaudal velocities extended from dark red for slow velocities to yellow for high ones (Fig 1).

Mean velocity measurements were obtained, at each cardiac phase, by drawing a region of interest on the color composite image corresponding to the total cyst and to the total PCSS areas in the patients and to the total perispinal subarachnoid spaces in the control group. Care was taken not to include periradicular epidural veins. Selected areas varied in the cysts from 0.05 to 1.83 cm^2. We used a modulus threshold in order to eliminate pixels of less than 5% intensity of the maximum intensity of the pixels in the slice. Velocity measurements were performed in the cysts and in the PCSS of the patients and were compared with the data collected in the subarachnoid spaces of the healthy subjects.

We measured the following parameters: 1) in the patient group: maximum systolic and diastolic cyst velocities, maximum systolic PCSS velocities, time of onset of maximum systolic cyst, and PCSS velocities as a percentage of the RR interval; 2) in the control group: maximum systolic and diastolic velocities in the subarachnoid spaces and time of onset of maximum velocity in the subarachnoid spaces. Mean and standard deviation on the previous parameters were obtained in the different groups. Statistical significance was calculated by means of a Student's *t* test. We considered a *P* value of less than .05 mandatory for statistical significance.

We compared velocity measurements with the clinical status of the patients and with the morphology of the cysts. All the patients underwent a complete clinical workup, providing information about the evolution of the disease and the clinical status at the moment of flow measurements. We used a clinical scale similar to the one proposed by Fischer and Brotchi (29) in the evaluation of patients with spinal cord tumors, and the each patients was classified into one of five groups:

- grade 0: no functional deficit, normal clinical examination
- grade 1: presence of functional and objective symptoms but with no effect on the familial or professional life of the patients.
- grade 2: presence of functional and objective symptoms with disturbance of the familial and/or professional life of the patients.
- grade 3: disability with conservation of self-reliance.
- grade 4: disability with loss of self-reliance.

All the patients underwent both a pre- and postoperative clinical evaluation. Preoperative axial and sagittal T1-weighted studies were performed, and the cysts were classified into four groups according to the craniocaudal extension of the cyst (CEC), and to the subarachnoid spaces (SAS) surrounding the cyst:

- group A: CEC ≥ 15 cm, SAS not visible around the cyst
- group B: 5 cm < CEC < 15 cm, compressed but still visible pericystic SAS
- group C: CEC ≤ 5 cm, normal pericystic SAS.
- group D: normal aspect of the spinal cord or simple cleft with no enlargement of the cord.

Degree of stenosis at the craniocervical level was scored as follows:

- bony stenosis: 2 points
- disappearance of the anterior SAS: 1 point
- morphology of the cisterna magna: partially compressed (1 point), not visible (2 points)
- degree of Chiari I malformation: C0-C1 (1point), C2 (2 points), >C2 (3 points).

Patients could then be classified in three groups:

- group 0, normal foramen: score = 0
- group 1, foramen partially occluded: score < 4
- group 2, foramen severely occluded: score ≥ 4

Clinical and morphologic data were compared with the cyst velocities by means of a dependent *t* test.

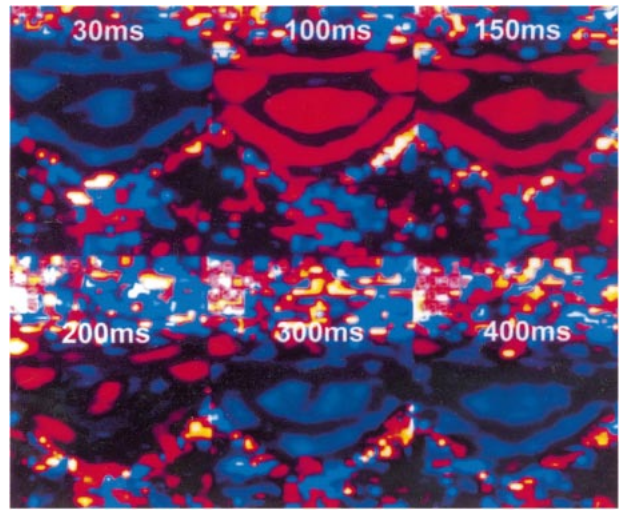

FIG 1. Cervical syringomyelia. Axial slice, preoperative velocity imaging (patient 11).

Six images are obtained 30, 100, 150, 200, 300, and 400 ms after the R-wave. Craniocaudal velocities are represented in red and caudocranial velocites in blue. A pulsatile flow is observed as well in the cyst as in the PCSS.

TABLE 1: Healthy volunteers

Subject (no.)	MSV (cm/s)	SP (%RR)	MDV (cm/s)
1	2.39	23	1.43
2	2.12	17	1.09
3	1.18	23	0.71
4	2.81	25	1.39
5	2.85	21	2.06
6	1.94	25	1.43
7	2.03	25	1.16
8	4.79	23	1.39
9	5.49	13	1.50
10	2.67	27	1.54
11	2.48	27	1.46
12	2.93	20	1.17
13	3.91	21	0.68
14	5.89	15	2.22
15	3.72	18	1.03
16	4.32	21	2.11
17	4.32	21	3.85
18	2.95	30	2.40
19	4.64	30	1.63

Note.—MSV = maximum systolic velocity, MDV = maximum diastolic velocity, SP = onset of the systolic peak formulated as a fraction of the RR-interval.

Results

Healthy Subjects

Thirty-six measurements of the spinal CSF velocity were available in the 19 volunteers. The dynamics of the CSF velocity has a typical waveform. It is characterized by a biphasic pattern. Immediately following the R-wave of the ECG, an ascending CSF flow is observed. Secondarily, flow direction promptly reverses and the CSF velocity curve is characterized by an always well-defined craniocaudal velocity peak, occurring during the first third of the RR cycle. Craniocaudal peak occurrence is synchronous to the carotid systolic peak. Afterward, an ascending flow is observed during the second half of the cardiac cycle.

Maximum systolic CSF velocities greatly differed from one volunteer to another and, in the same subject, from one cervical level to another. Results corresponding to the levels where higher SAS velocities were measured are summarized in Table 1. On the other hand, the systolic peak occurs in the first third of the RR cycle (21% RR, SD = 5%), whatever the level of the measurement (Fig 2). Maximum diastolic CSF velocities (1.49 ± .68 cm/s) were significantly ($P<.001$) lower than were systolic velocities (2.65 ±.1.65 cm/s), and no distinct diastolic peak was noted.

Patients

Clinical and morphologic data of the patients are provided in Table 2. Two patients (patients 4 and 16) had null cyst flow dynamics. These two patients had small cysts (graded B or C). In the 16 other patients, flow pattern inside the cyst was similar to the one observed in the SAS of the volunteers. A pulsatile flow was demonstrated in the cysts and PCSS with a craniocaudal systolic flow characterized by a well-defined systolic peak appearing in the first third of the RR duration and with a diastolic caudocranial flow.

In large cysts, higher velocities were observed in the center of the cyst. Maximum systolic and diastolic cyst velocities greatly differed from one patient to another. At the same cervical level, maximum mean systolic cyst velocities (1.97 ± 1.60 cm/s) were significantly ($P = .02$) higher than were diastolic cyst velocities (1.07 ± 0.63 cm/s). No statistically significant ($P = .36$) difference was observed in terms of maximum mean systolic velocities in the cyst (1.97 cm/s, SD = 1 .60 cm/s) and in the PCSS (1.80 cm/s, SD = 1.20 cm/s). At the same cervical level, the maximum systolic velocity peak occurred significantly ($P = .0003$) sooner in the cyst (21 ± 5% of the RR duration) than in the PCSS (28 ± 7 % of the RR duration).

A comparison between velocity measurements and cyst morphology was available in all the patients before surgery. Maximum mean velocities are significantly higher in large syrinxes (graded A or AB) than in small cysts (graded B or C) during

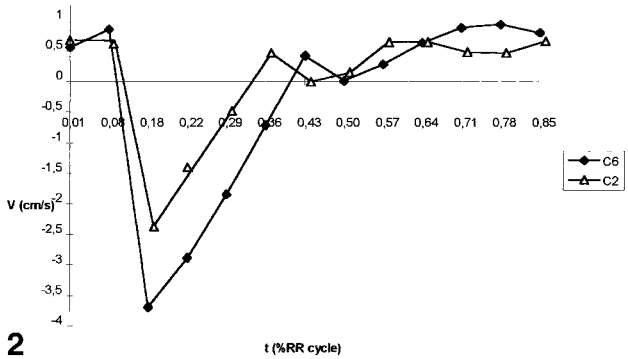

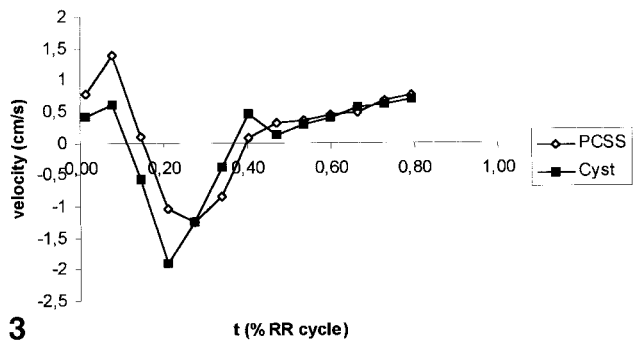

FIG 2. Normal kinetics of CSF at C2 and C6 levels (volunteer 15).
Caudal flow is represented by negative values. A systolic velocity peak is clearly defined, and it occurs in the first third of the RR cycle duration.

FIG 3. Cystic and pericystic kinetics (patient 1).
A systolic peak is observed in the PCSS and in the cyst, but it occurs sooner in the cyst.

TABLE 2: Pre- and postoperative evaluation of patients

Patient No.	Clinical Grade			Foraminal Stenosis		Cyst Distension		Cyst Velocities (cm/s)								PCSS Velocities (cm/s)				
								Systolic			S. Peak		Diastolic			Systolic			S. Peak	
	Pre-Op.	Post-Op.	Supra Spinal Deficit	Pre-Op.	Post-Op.	Pre-Op	Post-Op	Pre-Op.	Post-Op.	% Change	Pre-Op.	Post-Op.	Pre-Op.	Post-Op.	% Change	Pre-Op.	Post-Op.	% Change	Pre-Op.	Post-Op.
1	1	1	0	1	1	A	B	−1.90	−1.80	−5.3	0.21	0.27	0.69	0.78	13.0	−1.26	−1.43	11.9	0.27	0.27
2	2	2	N	2	0	A	C	−3.80	−0.85	−77.6	0.23	0.17	1.33	0.82	−38.3	0	−3.01	⋯	NS	0.37
3	0	0	N	2	0	A-B	A-B	−1.24	−0.85	−31.5	0.19	0.20	0.77	0.87	13.0	−2.71	−3.28	17.4	0.27	0.20
4	1	1	N, S, C	2	0	C	C	0	0	⋯	⋯	⋯	0	0	⋯	−3.48	−3.46	−0.6	0.37	0.24
5	1	1	N, V	2	2	A	A	−2.83	−2.01	−29.0	0.27	0.29	1.59	1.64	3.1	−1.85	−1.14	−62.3	0.27	0.29
6	2	1	N, C	2	2	B	B	−0.71	−1.09	53.5	0.21	0.21	1.34	1.29	−3.7	−2.51	−3.91	35.8	0.30	0.30
7	1	1	N	1	0	B	C	−1.07	0	−100	0.20	NS	0.76	NS	NS	−1.02	−2.17	53.0	0.38	0.39
8	0	0	0	2	0–1	B	C?	−0.46	0	−100	0.10	⋯	0.72	0	−100.0	−1.34	−1.86	28.0	0.19	0.20
9	3	3	N	1	0	A	B	−2.64	−3.20	21.2	0.17	0.20	1.76	1.35	−23.3	−1.2	−2.73	56.0	0.32	0.20
10	2	2	N, V	2	0	B	B	−0.52	−0.49	−5.8	0.20	0.20	0.51	1.04	103.9	−0.78	−1.03	24.3	0.20	0.20
11	1	1	0	1	0–1	A	C	−2.84	0	−100	0.20	⋯	2.23	0	100.0	−3.28	−1.66	−97.6	0.24	0.26
12	1	1	N	2	0	B	D	−0.45	0	−100	0.16	NS	0.48	0	100.0	−3.72	NS	⋯	0.30	NS
13	1	0.5	H, N	2	0	A	B	−2.79	−0.49	−82.4	0.20	0.20	0.94	0.42	−55.3	−1.09	−1.76	38.1	0.30	0.30
14	2	1	S	2	0	A	B	−6.21	−1.75	−71.8	0.23	0.20	2	1.94	−3.0	0	−0.68	⋯	NS	0.20
15	1	1	N	2	1	A	C	−2.67	−2.63	−1.5	0.21	0.19	1.35	1.67	23.7	−1.16	−1.54	24.7	0.41	0.27
16	1	0	0	2	0	B	D	0	0	⋯	NS	NS	0	0	⋯	−1.27	−1.31	3.1	0.29	0.11
17	1	1	0	1	0	A	C	−2.10	−1.45	−31.0	0.32	0.11	1.39	0.91	−34.5	−1.78	−3.2	44.4	0.25	0.20
18	2	2	V	2	1	A	B	−3.18	−2.43	−23.6	0.18	0.20	1.4	1.46	4.3	−3.87	−4.41	12.2	0.18	0.20

NB: Velocities are expressed in cm/s and time of occurrence of the systolic peak in % of the RR cycle duration. N = nystagmus, C = cerebellum deficit, S = swallowing troubles, V = velum paresis, H = hiccup. Modality of clinical grading and evaluation of the foraminal stenosis are explained in the text.

systole (2.93 cm/s ± 1.28 cm/s versus 0.46 ± 0.38 cm/s, $P = .00003$) and diastole (1.50 ± 0.57 cm/s versus 0.54 ± 0.47 cm/s, $P = .0008$). Conversely, PCSS velocities did not appear significantly ($P = .275$) different at the periphery of small syrinxes (2.02 ± 1.21 cm/s) and at the vicinity of large spinal cord cysts (1.65 ± 1.23 cm/s). Furthermore, time differences between the R-wave and the onset of the systolic peak is shorter in small cysts (17 ± 5 % RR versus 22 ± 4 % RR, $P = .05$).

There is no correlation between the duration of the clinical symptoms related to the cysts and the intensity of the velocities measured in the syrinxes and in the PCSS. Patients with high clinical score (2 or 3) presented significantly ($P = .05$) higher diastolic cyst velocities (1.39 cm/s, SD = 0.51 cm/s versus 0.91 cm/s, SD = 0.66 cm/s) than did patients with low clinical score (0 or 1). We failed to find any significant differences between maximum systolic cyst velocities, maximum systolic velocities in the PCSS time of onset of the systolic peak in the cyst, and in the PCSS of the two groups.

Fourteen patients presented with supraspinal symptoms (nystagmus, swallowing troubles, velum paresis). A Chiari I malformation may probably be responsible for most of these symptoms. We observed a significantly ($P = .02$) early occurrence of the systolic peak in the PCSS in patients with no supraspinal neurologic signs (24% RR versus 30% RR), but no difference concerning cyst or PCSS systolic velocities.

The mean interval between surgery and the postoperative study was 10.2 months (range, 1.4 to 55.2 months). Decrease in cyst velocity was observed after surgery (mean maximum systolic pressure: 1.97 cm/s, SD = 1.6 cm/s [preoperative] versus 1.26 cm/s, SD = 1.08 cm/s [postoperative], $P = .03$; mean maximum diastolic pressure: 1.07 cm/s, SD = 0.63 cm/s [preoperative] versus 0.83 cm/s, SD = 0.67 cm/s [postoperative], $P = .05$) (Fig 4). The decrease of mean maximum systolic cyst velocities was observed in 16 patients with a mean value of 42.8%. In two patients (patient 6 and 9), we observed an increase in systolic cyst velocities. Both presented with a large cyst (graded B) and one (patient 6) had an insufficient enlargement of the craniocervical foramen. In the PCSS, we observed in the postoperative course a parallel increase of systolic mean maximum velocities (2.27 cm/s, SD = 1.11 cm/s versus 1.8 cm/s, SD = 1.2 cm/s, $P = .01$) and an earlier occurrence of the systolic peak (25% RR, SD = 7% RR versus 28% RR, SD = 7% RR, $P = .02$).

After surgery, the patients were classified, according to the degree of enlargement of the craniocervical junction, in the two followings groups:

- group A: (patients 2–4, 7–14, 16, 17) with an effective enlargement of the craniocervical junction evaluated on sagittal T1-weighted MR images.
- group B: (patients 1, 5–6, 15, 18) with a doubtful efficacy of the surgical procedure.

We found in group A significantly lower systolic (0.72 cm/s versus 1.99 cm/s, $P = .01$) and diastolic (0.61 cm/s versus 1.37 cm/s, $P = .008$) cyst velocities. On the other hand, we found no difference between the two groups concerning systolic velocities in the PCSS, time of occurrence of the systolic peaks in the cysts, and in the PCSS.

Considering the cyst evolution in the postoperative course, we studied the velocity patterns in two groups of patients:

- group A (patient 1, 5, 9–11, 13, 14, 19, 23) with no major decrease or unchanged cyst volume.
- group B (patient 4, 8, 15–17, 20–22) with obvious collapse of the cyst.

Preoperative velocity patterns were elsewhere analogous in the two groups. Lower postoperative diastolic cyst velocities in group B (0.48 cm/s versus 1.15 cm/s) were the only significant ($P = .02$) difference observed between the two groups.

Discussion

Technical Considerations

Flow Measurement Technique.—Two principal flow measurement techniques have been described with MR imaging. The phase mapping (PM) method (12, 13, 30) is based upon the subtraction of a phase image obtained after flow compensation from a velocity-encoded phase image. FEVI consists of step-by-step increases in the amplitude of the velocity-encoding gradient (11, 16, 28). It is then possible to separate phase spatial inhomogeneities from flow-related phase by using Fourier transformation. FEVI, when associated with a zero-filling interpolation, is a precise method for velocity measurements, with a better signal-to-noise ratio than PM, even with a number of encoding steps reduced to four (28). Determination of null velocities with FEVI is unambiguous. With this small number of encoding steps, sequence durations of FEVI and PM are comparable.

Image Analysis.—Using a modulus threshold eliminates the very low intensity pixels, which chiefly correspond to noise, the phase angle of which is difficult to determine precisely. The level of the threshold was arbitrarily fixed at 5% of the maximum intensity of the pixels in the image. The threshold eliminates also the signal from spins with slow flow. This is why we used thin (5-mm) slices in the view of maximizing the in-flight effect. As opposed to sagittal in-plane flow measurement, measurement in the axial plane (through-plane) allows a truly quantitative approach of flow velocities in the entire syringomyelic cyst and in the PCSS. Partial volume error, owing to the thin slice thickness used in the study, is minimized.

FIG 4. Pre- and postoperative evolution (patient 13). Pre- and postoperative cyst morphology (*A*), pre- (*B*) and postoperative (*C*), velocity imaging, evolution of cyst (*D*), and of PCSS velocities (*E*) are shown. PCCS velocity increases in the postoperative course. In this case with a partial reduction of the cyst volume, cyst velocity distinctly decreases.

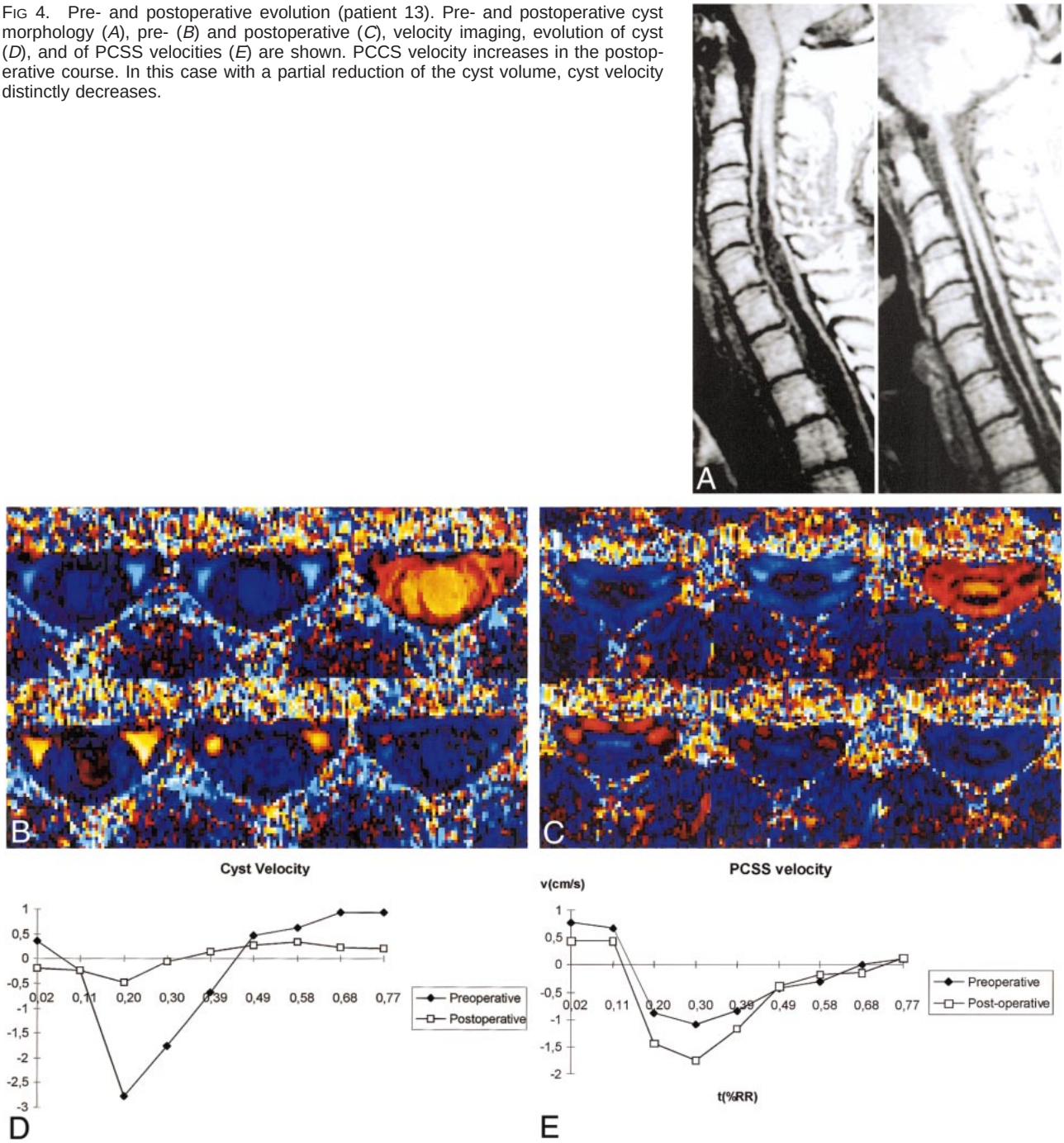

Pulsatile Pattern of the CSF.—Pulsatility of the CSF has been known for a long time and was initially demonstrated on the basis of myelographic studies (31, 32). It is related to choroid plexus pulsations (33) and is modulated by the respiratory cycle (34). Cine phase contrast flow study constitutes a valuable technique for imaging CSF pulsatile flow and may provide quantitative data (20, 24, 25, 35). Our results of velocity measurements in healthy subjects are consistent with those of previous studies (20, 25). A slight difference in the time of the systolic peak in healthy subjects is observed by several authors (25, 27). This is probably due to the different triggering technique.

Velocity Pattern in the Cysts and in the PCSS.—The pulsatile pattern of the contents of syringomyelic cysts has already been demonstrated with MR imaging (36) and may be revealed by T2-weighted spin-echo sequence withouts flow compensation. Dephasing of moving spins explains the signal intensity of pusatile cysts that appear dark on such sequences. Until now, the few studies of syringomyelia performed using phase-contrast imaging (17, 21) did not provide a quantitative analysis.

Our study confirms the pulsatility of cyst content and the persistence of a pulsatile pattern in the PCSS of the patients. An earlier occurrence of the sytolic peak in the cyst when compared with that in the PCSS was observed. These findings may suggest that there is no major obstacle to the fluid circulation inside the cyst cavity and that the time of onset of the systolic peak in the CSF of volunteers and in the cyst of the patients is similar. Aboulker (1) emphasized the fact that the syrinx is usually not distended but is more often a flaccid fluid collection. We can then imagine that the progressive filling of the cyst during the systolic wave may then constitute a progressive obstacle to the PCSS flow, which is reflected by a delay in the onset of the PCSS systolic peak. The lower resistance to fluid circulation inside the syrinx (assessed by a faster occurrence of the systolic peak in the cyst) is probably of great interest if we consider new theories of the pathogenesis of syringomyelia. It is postulated that the spinal subarachnoid space is normally anatomically continuous with the central canal and that the formation of noncommunicating syrinxes may depend upon the association of the obstruction of the CSF pathways with a variable degree of stenosis of the central canal (37, 38). One can assume that high cyst velocities observed in large cysts constitute an indirect consequence of the obstruction of the PCSS if we consider the spinal cord and the central canal as the vehicles through which there is flow of CSF (1, 37, 38) from the spinal subarachnoid spaces, through the Virchow-Robin spaces.

We observed a decrease in both rostral (systolic) and caudal (diastolic) cyst flow after enlargement of the craniocervical junction. The earlier occurrence of the PCSS systolic peak in the postoperative period is indicative of the diminution of the impedance of the SAS, which is probably related to 1) spinal canal enlargement and 2) the decrease of a dynamic impedance relative to the progressive filling of the syrinx during the cardiac cycle.

Oldfield et al (5) proposed that the rapid caudal tonsillar movements observed during systole in patients with Chiari I malformation act as a piston and may be responsible for an accentuated systolic pressure wave, forcing CSF into spinal cord parenchyma. After surgery, we observed an increase of the PCSS velocities, probably reflecting canal decompression. This point was already shown by Bhadelia et al (26), who reported improvement of systolic CSF flow pulsations immediately below the foramen magnum. We thus consider that *low preoperative PCSS systolic velocities,* when compared with the velocities observed after surgery, are probably unlikely with *high preoperative systolic pressure of the PCSS.*

An important point to consider is the intensity of *diastolic cyst velocities.* In the preoperative period, higher diastolic velocities are observed 1) in larger cysts and 2) in patients with a poor neurologic status. After surgery, they are noted 1) in patients with incomplete canal enlargement and 2) in patients with incomplete cyst collapse. Milhorat et al (39) already emphasized the rostral direction of CSF flow through the central canal in rats. Fischbein et al (37) hypothesized that, in the presence of a Chiari I malformation, CSF may be driven into the spinal cord through the perivascular spaces because of the high pressure of the PCSS during systole. Nevertheless, our study led us to consider that this phenomenon is probably independent from PCSS systolic hyperpressure. We postulate, then, that the net flow to the central canal is dependent on canal obstruction *during diastole.* In the same way, it is interesting to consider the concept of a ''presynrix state'' (37). In the five patients included in Fischbein et al's study, the cervical cord T2 prolongations observed were visible *immediately below* the presumed level of the canal stenosis.

As the central canal is usually partially obliterated, the location and the extension of the syrinx are probably defined by focal canal stenosis. It is also possible that tonsillar ectopia acts both on the foraminal level and the central canal by compressing them peculiarly during the abrupt downward tonsillar movements observed during systole (5).

Concerning the progressive extension of cyst volume in syringomyelia, we think that high systolic cyst velocity may then account for caudal extension of the cyst. In the same way, high diastolic cyst velocity, probably in relation with the canal stenosis, may also explain the cranial extension of the syrinx.

Conclusion

Our study demonstrates impaired CSF flow pulsations in patients with syringomyelia. A quantitative approach of the kinetics of the cyst and the PCSS has demonstrated that cyst velocities seem to depend on clinical progression and cyst morphology. Velocity modifications induced by surgery are consistent with a reduction of the impedance of PCSS. CSF flow imaging does constitute a direct evaluation for the follow-up and the postoperative survey in patients with syringomyelic cysts. Diastolic cyst flow seems to be of critical importance in the extension of syringomyelic cysts. After surgery, high diastolic cyst velocities have to be considered as indicative of a poor operative result.

References

1. Aboulker J. **La syringomyélie et les liquides intra-rachidiens.** *Neurochirurgie* 1979;25:1–115
2. Ball MJ Dayan AD. **Pathogenesis of syringomyelia.** *Lancet* 1972; 2:799–801
3. Gardner W. **Hydrodynamic mechanism of syringomyelia: its relationship to myelocele.** *J Neurol Neurosurg Psychiatry* 1965;28: 247–259
4. Williams B. **The distending force in the production of "communicating syringomyelia."** *Lancet* 1969;2:696–697
5. Oldfield EH, Muraszko K, Shawker TH Patronas NJ. **Pathophysiology of syringomyelia associated with Chiari I malformation of the cerebellar tonsils: implications for diagnosis and treatment.** *J Neurosurg* 1994;80:3–15

6. Stoodley MA, Brown SA, Brown CJ Jones NR. **Arterial pulsation-dependent perivascular cerebrospinal fluid into the central canal in the sheep spinal cord.** *J Neurosurg* 1997;86:686–693
7. Stoodley MA, Jones NR Brown CJ. **Evidence for rapid fluid flow from the subarachnoid space into the spinal cord central canal in the rat.** *Brain Res* 1996;707:155–164
8. Milhorat TH, Nobangedani F, Miller JI, Rao C. **Noncommunicating syringomyelia following occlusion of central canal in rats.** *J Neurosurg* 1993;78:274–279
9. Feinberg DA, Crooks LE, Hoenninger J. **Pulsatile blood velocity in human arteries displayed by MRI.** *Radiology* 1984;153:177–180
10. Firmin DN, Nayler GL, Klipstein RH. **In vivo validation of MR velocity imaging.** *J Comput Assist Tomogr* 1987;13:751–756
11. Hennig J, Muri M, Brunner P. **Quantitative flow measurement with the fast fourier flow technique.** *Radiology* 1988;166: 237–240
12. Meier D, Maier S, Böesiger P. **Quantitative flow measurements on phantoms and on blood vessels with MR.** *Magn Res Med* 1988;8:25–34
13. Nayler GL, Firmin DN, Longmore DB. **Blood flow imaging by cine magnetic resonance.** *J Comput Assist Tomogr* 1986;10:715–722
14. Ciraolo L, Mascalchi M, Bucciolini M. **Fast multiphase MR imaging of aqueductal CSF flow: study of healthy subjects.** *AJNR Am J Neuroradiol* 1990;11:589–596
15. Enzmann DR, Pelc NJ. **Normal flow patterns of intracranial and spinal CSF defined with phase contrast cine MR imaging.** *Radiology* 1991;178:467–474
16. Feinberg DA, Mark AS. **Human brain motion and CSF circulation demonstrated with MR velocity imaging.** *Radiology* 1987;163:793–799
17. Levy LM, Di Chiro G. **MR phase imaging and CSF flow in the head and spine.** *Neuroradiology* 1990;32:399–406
18. Martin AJ, Drake JM, Lemaire C. **Cerebrofluid shunts: flow measurements with MR imaging.** *Radiology* 1989;173:243–247
19. Mascalchi M, Ciraolo L, Tanfani G. **Cardiac-gated phase MR imaging of aqueductal CSF flow.** *J Comput Assist Tomogr* 1988; 12:923–926
20. Nitz WR, Bradley WG, Watanabe AS. **Flow dynamics of CSF fluid: assessment with phase-contrast velocity MR imaging performed with retrospective cardiac-gating.** *Radiology* 1992; 183:395–405
21. Quencer M, Donovan Post MJ, Hinks RS. **MR imaging in the evaluation of normal and abnormal CSF flow: intracranial and intraspinal studies.** *Neuroradiology* 1990;32:371–391
22. Ridgway JP, Turnbull LW, Smith MA. **Demonstration of pulsatile cerebrospinal fluid flow using magnetic resonance phase imaging.** *Br J Radiol* 1987;60:423–427
23. Thomsen C, Stahlberg F, Stubgaard M. **Fourier analysis of CSF flow velocities: MR imaging study.** *Radiology* 1990;177:659–665
24. Henry-Feugeas MC, Idy-Peretti I, Blanchet B. **Temporal and spatial assessment of normal cerebrospinal fluid dynamics with MR imaging.** *Magn Reson Imaging* 1993;11:7–12
25. Bhadelia RA, Bogdan AR, Wolpert SM. **Analysis of cerebrospinal fluid flow waveforms with gated phase-contrast MR velocity measurements.** *AJNR Am J Neuroradiol* 1995;16:389–400
26. Bhadelia RA, Bogdan AR, Wolpert SM. **Cerebrospinal fluid flow waveforms: analysis in patients with Chiari I malformation by means of gated phase-contrast MR imaging velocity measurements.** *Radiology* 1995;196:195–202
27. Wolpert SM, Bhadelia RA, Bogdan AR. **Chiari I malformations: assessment with phase-contrast velocity MR.** *AJNR Am J Neuroradiol* 1995;15:1299–1308
28. Bittoun J, Bourroul E, Jolivet O, Idy-Peretti I. **High precision MR velocity mapping by 3D-Fourier phase encoding with a small number of encoding steps.** *Magn Reson Med* 1993;29:674–680
29. Fischer G, Brotchi J. **Intramedullary spinal cord tumors. Report. French Society of Neurosurgery. 45th annual congress.** *Neurochirurgie* 1994;40:1–108
30. Bryant DJ, Payne JA, Firmin DN. **Measurement of flow with NMR imaging using a gradient pulse and phase difference technique.** *J Comput Assist Tomogr* 1984;8:588–593
31. DuBoulay GH. **Pulsatile movements in the CSF pathways.** *Br J Radiol* 1966;39:255–262
32. Gilland O, Chin F, Anderson WB. **A cinemyelographic study of cerebrospinal dynamics.** *AJR Am J Roentgenol* 1969;106:369–375
33. Bering EAJ. **Choroid plexus and arterial pulsation of cerebrospinal fluid: demonstration of the choroid plexuses as a cerebrospinal pump.** *Arch Neurol Psychiatr* 1955;73:165–172
34. Adolph R, Fukusumi H, Fowler N. **Origin of cerebrospinal pulsations.** *Am J Physiol* 1967;212:840–846
35. Enzmann DR, Pelc NJ. **Normal flow patterns of intracranial and spinal cerebrospinal fluid defined with phase-contrast cine MR imaging.** *Radiology* 1991;178:467–474
36. Enzmann DR, O'Donohue J, Rubin JB. **CSF Pulsations within nonneoplastic spinal cord cysts.** *AJNR Am J Neuroradiol* 1987; 8:517–525
37. Fischbein NJ, Dillon WP, Cobbs C, Weinstein PR. **The "presyrinx" state: a reversible myelopathic condition that may precede syringomyelia.** *AJNR Am J Neuroradiol* 1999;20:7–20
38. Milhorat TH. **Is reversible enlargement of the spinal cord a presyrinx state?** *AJNR Am J Neuroradiol* 1999;20:21–22
39. Milhorat TH, Johnson RW, Johnson WD. **Evidence of CSF flow in rostral direction through central canal of spinal cord in rats.** In: Matsumoto N, Tamaki N, eds. *Hydrocephalus: Pathogenesis and treatment.* Tokyo: Springer-Verlag;1992;:207–217